Environmental Research 202 (2021) 111517

Contents lists available at ScienceDirect

Environmental Research

journal homepage: www.elsevier.com/locate/envres

Electrochemical and sonochemical advanced oxidation processes applied to tartrazine removal. Influence of operational conditions and aqueous matrix

G. Donoso [a], Joaquin R. Dominguez [a], T. González [a], S. Correia [a], Eduardo M. Cuerda-Correa [b,*]

[a] Department of Chemical Engineering and Physical Chemistry. Area of Chemical Engineering. Faculty of Sciences, University of Extremadura, Avda. de Elvas, s/n, E-06006, Badajoz, Spain

[b] Department of Organic and Inorganic Chemistry. Faculty of Sciences, University of Extremadura, Avda. de Elvas, s/n, E-06006, Badajoz, Spain

ARTICLE INFO

Keywords:
Electrochemical oxidation
Sonochemical oxidation
Tartrazine
Boron doped diamond electrodes
Optimization

ABSTRACT

Tartrazine degradation was investigated by electrochemical and sonochemical oxidation processes. Anodic oxidation was carried out using boron-doped diamond (BDD) electrodes. The influence of current density and dye initial concentration on the removal of tartrazine from water was analyzed. The experimental results indicate that total removal of tartrazine was obtained, and Chemical Oxygen Demand (COD) and Total Organic Carbon (TOC) removals of up to 94.4% and 72.8% were achieved, respectively. To optimize the process, the pollutant removal percentage, the kinetic rate constant, and the TOC removal efficiency were chosen as target variables. Moreover, sonochemical oxidation experiments at a high-frequency range of cavitation (up to 1 MHz) were performed to establish the influence of three different operating variables, namely ultrasound frequency (0.5–1.1 MHz), ultrasound power (2.0–26.6 W $\cdot L^{-1}$), and pulse-stop ratio (5:1–1:1). The process was also analyzed in terms of kinetics and energy costs. The kinetics resulted to be three times faster for the electrochemical process. However, the calculated energy costs were very similar, at least at long treatment times. Finally, the influence of three aqueous matrices was investigated. According to the experimental results, the natural occurrence of chloride and/or nitrate ions in water strongly conditions the rate of the process, although at least 90% of tartrazine removal was achieved within the first 50 min of treatment.

1. Introduction

In recent years a growing concern has arisen in connection with the effect of dyes on terrestrial and aquatic ecosystems (Collivignarelli et al., 2019; Srinivasan and Sadasivam, 2021) as well as on human health. The presence of azo dyes even at low concentrations is recognized as causing harmful health impacts (Raza et al., 2021), as many of them may lead to carcinogenic, mutagenic, or allergic reactions (Gicevic et al., 2020; Sahnoun and Boutahala, 2018; Rovira and Domingo, 2019). As a result, many countries such as the USA, the European Union (EU), and international organizations as the World Health Organisation (WHO) have developed laws and regulations to prevent the indiscriminate use of dyes as food additives.

Tartrazine ($C_{16}H_9N_4Na_3O_9S_2$), also known as Acid Yellow 23 (AY 23), CI 19140 or E102 additive, is an azo dye used in the food industry, to confer bright yellow or orange color to a variety of food products, as well as in the cosmetics and textile industry (Tekin et al., 2018). However, in the last decade, clinical pieces of evidence on the potential toxicity of tartrazine on humans have been found (Mpountoukas et al., 2010; Amchova et al., 2015; Khayyat et al., 2017; Floriano et al., 2018), so that its use as a food additive is prohibited in Norway and is controversial in the European Union and the United States.

The removal of tartrazine from water and wastewater is far from being simple and requires the application of severe methods. These methods include electro-oxidation (EO), also called anodic oxidation or electrochemical incineration (Candia-Onfray et al., 2018; Ouarda et al., 2019; Zhang et al., 2013). EO involves the oxidation of contaminants in an electrolytic cell by direct transfer of electrons to the anode, and indirect or mediated oxidation by oxidizing species generated from the electrolysis of water (mainly by the physisorbed HO· radicals) (Panizza and Cerisola, 2009) or generated *in situ* (e.g., persulfates, peroxophosphates, ferrates, chlorine, etc.) due to the high oxidation capacity of the hydroxyl radical (Cai et al., 2018; da Silva et al., 2018; Ghasemian et al., 2017; Nakamura et al., 2019). EO constitutes a promising alternative for the control of industrial wastewater pollution (Weng and Pei, 2016). Excellent removal efficiencies of a wide variety of contaminants

* Corresponding author.
E-mail address: emcc@unex.es (E.M. Cuerda-Correa).

https://doi.org/10.1016/j.envres.2021.111517
Received 17 March 2021; Received in revised form 3 June 2021; Accepted 3 June 2021
Available online 30 June 2021

can be achieved by EO (Urtiaga et al., 2013).

It has been shown that the presence of these species exerts a significant effect on increasing the oxidation capacity of the system (Rodrigo et al., 2010). Very often, the simultaneous presence of different oxidizing species has a synergistic effect, thus improving the removal of contaminants and giving rise to high mineralization rates (Canizares et al., 2007, 2008).

Feng et al. (2013) showed the main mechanisms to be considered in anodic oxidation, and Comninellis (1994) described two types of anodes, *active* and *non-active*. At the anode (M), the oxidation of water, and the generation of hydroxyl physisorbed radicals, M (HO·), Eq. (1), take place.

$$M + H_2O \longrightarrow M(HO\cdot) + H^+ + e^- \quad (1)$$

In the case of active anodes, this radical strongly interacts with the surface and is transformed into chemisorbed *active oxygen* or superoxide, MO, Eq. (2).

$$M(HO\cdot) \longrightarrow MO + H^+ + e^- \quad (2)$$

The MO/M pair acts as a mediator in the electrochemical conversion of organic compounds, R, Eq. (3).

$$MO + R \longrightarrow M + RO \quad (3)$$

In contrast, the non-active anodes interact weakly with the hydroxyl radicals, so that HO· reacts directly with the organic products until total mineralization. Some metal oxides (e.g., PbO_2 and/or SnO_2) and, more specifically, boron-doped diamond (BDD) electrodes are considered as non-active anodes that promote the mineralization of pollutants. This process is usually limited by the matter transport and usually gives rise to total mineralization of the pollutant (Baluchova et al., 2019; Pereira et al., 2018; Sousa et al., 2019). It has also been suggested that other oxidizing species are formed along the process, such as heterogeneous HO·, Eq. (1), H_2O_2 (from HO· dimerization, according to Eq. (4), or O_3, by the breakdown of water on the surface of the anode, Eq. (5). However, physisorbed HO· is the most powerful oxidizing species among all of the above mentioned.

$$2M(HO\cdot) \longrightarrow 2MO + H_2O_2 \quad (4)$$

$$3H_2O \longrightarrow O_3 + 6H^+ + 6e^- \quad (5)$$

Boron Doped Diamond anodes have been widely used in water treatment due to their good chemical and electrochemical stability, inert surface, weak adsorption properties, long lifetime, and wide potential window (Hupert et al., 2003; Iniesta et al., 2001). It has been shown that many recalcitrant compounds, including phenols, chlorophenols, nitrophenols, pesticides, synthetic dyes, pharmaceuticals, and industrial leachates can be fully mineralized, with high current efficiency (Barrera et al., 2019; Bensalah and Bedoui, 2017; Frontistis et al., 2018; Marmanis et al., 2016).

Another attractive alternative for the removal of organic pollutants from water and wastewater is sonochemical oxidation (SO). In fact, the use of sonochemical oxidation as an auxiliary technique in wastewater treatments has been studied for several decades (Gogate, 2002). Sonochemistry is the branch of chemistry that studies the chemical and physical processes that take place in solution mediated by energy provided by ultrasound. The frequency ranges that are commonly used fall within 20 kHz to 2 MHz (Chatel and Colmenares, 2017). Among the various phenomena that appear in water when an ultrasound field is applied, the ultrasonic cavitation is to be highlighted. Cavitation is defined as the phenomenon of formation, growth, and implosion of microbubbles within the fluid that takes place in a very short interval of time (milliseconds) and releases a large amount of energy (Jagannathan et al., 2013).

Cavitation activity depends largely on the sonicator's parameters. Ultrasound efficiency is influenced by the frequency and power of the ultrasonic field, presence of dissolved gases and particles, physical properties of the solvent (volatility), temperature, reactor geometry (standing or progressive wave), etc. During this process, it is possible to generate, locally and in a very short time, temperatures close to 5000 K and extremely high pressures (180 MPa) inside the bubbles. Under these particular conditions, it is possible to carry out extremely difficult chemical reactions.

An aqueous solution in which cavitation takes place can be assimilated to an environment full of chemical micro-reactors where at least the sonolysis of water is carried out (i.e. the homolytic rupture of the molecule into HO· and ·H radicals) (Asgari et al., 2020). The subsequent participation of these radicals, especially the HO· radicals, in the oxidation of toxic and dangerous molecules, allows removing these contaminants (Pang et al., 2011). Thus, the degradation of organic compounds can take place by the action of hydroxyl radicals (oxidation mechanism) or due to high temperatures (pyrolytic mechanism). As a rule, oxidation is the most common degradation mechanism of hydrophilic and non-volatile species (e.g., dyes) whereas thermal degradation is more feasible for hydrophobic and volatile compounds.

In this work, the removal of tartrazine in water through electrochemical and sonochemical processes is presented, with the main focus on the influence of experimental conditions on the removal rate and efficiency both, in ultrapure and real water matrices.

2. Experimental

2.1. Material and reagents

Tartrazine ($C_{16}H_9N_4Na_3O_9S_2$, M_w = 534.36 g·mol^{-1}, CAS Number: 1934-21-0, purity ≥ 85.0%) was supplied by Sigma-Aldrich. For the electro-oxidation experiments, anhydrous sodium sulfate (M_w = 142.04 g·mol^{-1}, CAS Number: 7757-82-6, purity ≥ 99.0%) was also purchased from Sigma-Aldrich. All the solutions were prepared using ultrapure water obtained from a Millipore^{TM} Milli-Q Academy membrane purification system.

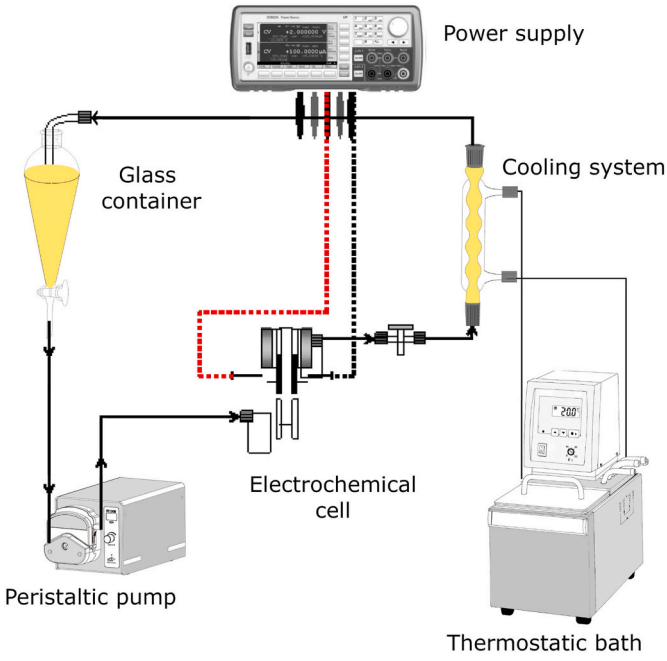

Fig. 1. Experimental setup for the electro-oxidation experiments.

2.2. Electro-oxidation process with boron-doped diamond electrodes

2.2.1. Experimental setup

The electro-oxidation experimental setup is depicted in Fig. 1. An experimental procedure previously described elsewhere (Dominguez et al., 2016; Palo et al., 2014; Gonzalez et al., 2011) was followed. Briefly, a single-compartment two-electrode electrochemical cell (Adamant Technologies, CSEM SA, Switzerland) was used. A boron-doped diamond (BDD) electrode was used as the anode, and a stainless steel (AISI 304) electrode acted as the cathode.

According to the provider's technical specifications, to prepare the BDD electrodes, a 2 mm thick silicon plate (p-silicon, 100 mΩ·cm) was coated with a thin (1 μm) boron-doped diamond (BDD) coating (100–150 mΩ·cm). Both electrodes were circular (φ = 10 cm, area = 78.54 cm^2) and the distance between the anode and the cathode was equal to 0.9 cm, thus yielding a total reactor volume equal to 70.69 cm^3. Efficient electrical connection was ensured by two adaptable copper current feeding electrodes and 4 mm diameter connectors. The electrodes were connected with the current feeding electrodes with the aid of a commercially available silver paste. A controlled DC power supply FA-665 (Promax, Ltd., Spain) was used. The maximum current intensity provided by the power supply was 20A, which leads to a maximum current density equal to 254.65 mA $\cdot cm^{-2}$.

The reactor was equipped with a cooling system with water inlet and outlet coupled to a thermostatic bath (Digiterm 100, JP Selecta, Barcelona, Spain) so that temperature was kept constant at 20 °C along all the experiments.

A 0.6 L glass container was used to feed the electrochemical cell with the tartrazine solution under a constant flux equal to 249 mL $\cdot min^{-1}$ with the aid of a peristaltic pump (Percom N-M, JP Selecta, Barcelona, Spain).

All the electro-oxidation experiments were conducted under the galvanostatic mode. The initial concentration of tartrazine ranged between 3 and 53 mg $\cdot L^{-1}$ (i.e., 0.56–9.92 $\cdot 10^{-5}$ M). Sodium sulfate was used as the supporting electrolyte at a concentration equal to 0.05 M.

2.2.2. Experimental design

In order to analyze the influence of two operational variables, namely, current density (j), and pollutant concentration in solution, (C) a factorial, composite, central, orthogonal, and rotatable (FCCOR) experimental design was used. The experimental design consists of 4 factorial experiments, 4 axial experiments, and 8 replicates of the central experiments, thus giving rise to an experimental matrix of 16 experiments. The coded and real values of the operational variables for each experiment are listed in Table 1.

2.3. Sonochemical oxidation

2.3.1. Experimental setup

The sonochemical oxidation experimental setup is depicted in Fig. 2. Briefly, a Meinhardt Multifrequency High Power System MFG generator (578, 860, and 1140 kHz) with variable power and pulse-stop relation time together with a Titanium flat transducer (75 mm diameter) was used to generate ultrasounds. A peristaltic pump (Percom N-M, JP Selecta, Barcelona, Spain) was used to make the tartrazine solution circulate through the ultrasound reactor (solution flux = 280 mL $\cdot min^{-1}$). The system was kept at constant temperature (namely, 20 °C) with the aid of a thermostatic bath (Digiterm 100, JP Selecta, Barcelona, Spain) coupled to the cooling jacket of the US reactor. In all experiments, 0.5 L of 5 $\cdot 10^{-5}$ M tartrazine solution was used.

2.3.2. Experimental procedure

The influence of three operating variables, namely, frequency (f), power (w) and pulse-stop ratio (p-s) on the pollutant removal efficiency was studied. Frequencies ranged from 578 up to 1140 kHz, whereas power values comprised between 2.0 and 26.6 W $\cdot L^{-1}$ were used. Finally, four different pulse-stop ratios were used in this study, too. It is worth noting that the operational variables cannot be modified to fit all

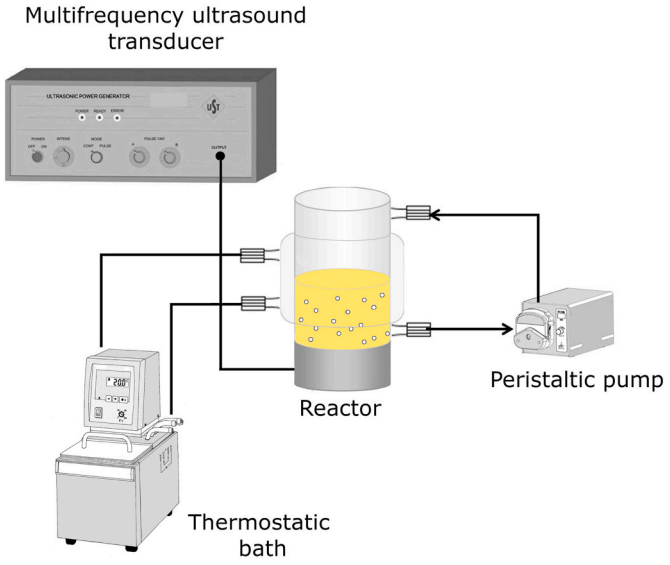

Fig. 2. Experimental setup for the sonochemical oxidation experiments.

Table 1
Experimental design matrix for the electro-oxidation of tartrazine with BDD electrodes. Treatment time was 120 min in all cases.

Experiment	Coded values		Real values		Dye removal (%)	TOC removal (%)	k_r min^{-1}
	j	C	j (mA $\cdot cm^{-2}$)	C (mg $\cdot L^{-1}$)			
1	1	−1	55.30	10.32	99.63	66.68	0.0978
2	0	0	34.00	28.00	99.70	72.90	0.0817
3	0	1.414	34.00	53.00	99.34	74.64	0.0488
4	0	0	34.00	28.00	99.79	73.10	0.0843
5	−1.414	0	3.88	28.00	57.85	35.60	0.0071
6	0	0	34.00	28.00	99.74	72.87	0.0816
7	−1	−1	12.70	10.32	98.93	36.37	0.0547
8	−1	1	12.70	45.68	90.55	64.07	0.0191
9	1.414	0	64.12	28.00	99.97	80.67	0.1418
10	0	−1.414	34.00	3.00	99.77	74.82	0.0880
11	0	0	34.00	28.00	99.63	72.80	0.0881
12	0	0	34.00	28.00	99.72	72.90	0.0814
13	0	0	34.00	28.00	99.71	72.70	0.0817
14	0	0	34.00	28.00	99.75	73.00	0.0835
15	0	0	34.00	28.00	99.70	72.80	0.0819
16	1	1	55.30	45.68	99.94	86.86	0.0879

the values necessary to perform an FCCOR design of experiments in a precise manner, due to technical limitations of the equipment. Hence, the operational variables were changed"“one at a time"'. The treatment time was 30 min in all cases. The experimental conditions for each experiment are listed in Table 2. Sonochemical efficiency was calculated as described by Koda et al. (2003).

2.4. Analytical methods

In order to determine the concentration of tartrazine present in the samples, an ultraviolet–visible spectrophotometric method was used. An Evolution 300 UV–Vis spectrophotometer (Thermo Scientific, Waltham, Massachusetts, USA) and quartz cuvettes of 1 cm optical path length were used. In all cases, ultrapure water was used as a reference (blank). A series of solutions of known tartrazine concentration ranging from 5.5 $\cdot 10^{-6}$ up to 1.1 $\cdot 10^{-4}$ mol $\cdot L^{-1}$ (i.e., 3–60 mg $\cdot L^{-1}$ were prepared and its UV–vis absorption was registered at λ_{max} = 428 nm. From the corresponding calibration curve (r^2 = 0.999), the molar extinction coefficient, ε, equal to 21761, was obtained. In the experiments carried out using different real waters, the calibration curve and all the spectrophotometric measurements were collected using the same aqueous matrix as the reference.

COD was determined with the aid of a Hanna Instruments HI 83099 photometer within a concentration range comprised between 0 and 150 mg $O_2 \cdot L^{-1}$. A Lange DR-2800 photometer was used to determine TOC in the concentration range 3–30 mg C $\cdot L^{-1}$. Specific commercially available cuvettes were used for COD and TOC determinations. The total content of phosphorus and nitrogen, as well as nitrate, nitrite, and ammonium, were determined using commercial kits and provided by Hanna Instruments Spain (Eibar, Guipuzcoa, Spain) and a HI83399 photometer.

3. Results and discussion

3.1. BDD electrochemical oxidation process

Table 1 summarizes the experimental results obtained in the BDD electrochemical oxidation process of tartrazine after 120 min of treatment time. In this work, the influence of current density (j) and initial concentration of pollutant (C) on three target variables (namely, the removal efficiencies of tartrazine and TOC, and the removal rate constant) has been studied. In the following sections, each of the target variables are firstly discussed separately, and, next, the process has been optimized in terms of removal efficiency and rate constant simultaneously.

3.1.1. Study of the tartrazine removal efficiency as the target variable

As indicated above, a Factorial, Composite, Central, Orthogonal, and Rotatable design of experiments has been used to study the influence of current density and tartrazine concentration on the removal efficiency of the dye. Table S1 (Supplementary Material) summarizes the results obtained in the analysis of variance (ANOVA) of the experimental data for tartrazine removal (%). All factors exhibiting a p-value below 0.05 exert a significant influence on the removal efficiency of the dye. As can be seen, in this case, the current density (A) and its squared value (AA) significantly influence the target variable with a probability of 95%. The Pareto plot shown in Fig. S1, top (Supplementary Material) confirms this assertion since the horizontal bars corresponding to A and AA exceed the vertical rule located around 2, which marks the significance of the effect. The main effects plot shown in Fig. S1, bottom (Supplementary Material) depicts the effect that each operational variable exerts on the target variable separately. It is foreseeable that an increase in current density results in a higher removal efficiency of tartrazine since the generation of HO· radicals on the anodic surface increases as the current density

Table 2
Experimental conditions and removal efficiencies for the sonochemical oxidation of tartrazine. f = frequency; w = power; p-s = pulse-stop ratio. Treatment time was 30 min in all cases.

Experiment	f (kHz)	w (W $\cdot L^{-1}$)	p-s (ms)	Removal efficiency (%)
1	578	26.6	250-50	31.4
2	578	10.9	250-50	28.2
3	578	2.0	250-50	6.0
4	578	10.9	100-100	18.4
5	860	10.9	100-100	19.4
6	1140	10.9	100-100	18.0
7	578	10.9	250-250	18.3
8	578	10.9	100-50	22.6

does. For instance, Kenova et al. (2018) obtained similar results in the electrochemical degradation of Mordant Blue 13 azo dye. However, from Fig. S1 it can be stated that the current density positively influences the removal efficiency of tartrazine until a maximum is reached. From this optimal value, a subsequent increase in j results in a rapid decrease in the removal efficiency. Since the pioneering works of Panizza et al. (2001a,b), and Rodrigo et al. (2001) till nowadays this behavior has been repeatedly described (Mousset et al., 2019; Barbosa et al., 2018; Scialdone et al., 2011; Palma-Goyes et al., 2010). In this connection, Panizza et al. (2001b) defined the so-called *limiting current density*, j_{lim}. According to these authors, when the system operates under galvanostatic conditions -as it is the case in the present study-two different regimes can be described:

- If $j < j_{lim}$ it may be stated that the electrolytic process is governed by the current, and organic intermediates are formed during the oxidation. This behavior persists until the applied current density equals the limiting current density
- If $j > j_{lim}$ the electrolytic process is mainly conditioned by mass transport phenomena, and organic compounds are completely mineralized to CO_2. Under these circumstances, secondary reactions (such as oxygen evolution or electrolyte decomposition) take place and a decrease in current efficiency is observed.

Another possible reason that may justify the negative effect of high values of current density is the generation of large amounts of $H_{2(g)}$ bubbles in the cathode from a given value of current density. This could adversely affect the oxidation process in the aqueous phase, as previously noted in other works of our research group (Dominguez et al., 2010, 2016; Palo et al., 2014; Gonzalez et al., 2011). All the exposed is in good agreement with the Pareto plot shown in Fig. S1, top (Supplementary Material). In fact, both the current density and the squared current density exert a significant influence on the removal efficiency of dye. However, the manner in which these two variables influence the removal efficiency is the opposite. It can be observed that the current density exerts a positive influence on the removal efficiency whereas the squared term of current density (i.e., high values of j) negatively influences the target variable. Fig. S1 (Supplementary Material) also depicts the influence of the initial concentration of dye on the removal efficiency of tartrazine. It can be observed that this factor has a much more limited impact on the removal efficiency than j. As expected, as the initial concentration of pollutant increases, the removal efficiency decreases, although to a limited extent. This fact is attributable to the presence of larger amounts of dye that must react with a constant quantity of hydroxyl radicals that are generated in solution. The use of the statistical design of experiments makes it possible to fit the experimental data to an equation that correlates the target variable with the operational ones. In a quadratic design, such an equation corresponds to a second-degree polynomial function, as illustrated in Eq. (6).

$$Pollutant\ removal\ efficiency\ (\%) = 99.7175 + 8.70709 \cdot j - 1.08477 \cdot C - -8.39627 \cdot j^2 + 2.1725 \cdot j \cdot C + 1.92628 \cdot C^2 \quad (6)$$

The positive or negative sign behind each of the coefficients included in this equation indicates the favorable or unfavorable influence of each variable, interaction, or squared term on the removal efficiency of the pollutant (%). The greater the absolute value of the coefficient, the greater the influence of that particular factor on the target variable. From multiple regression analysis, the response surface and contour curves depicted in Fig. 3 can be obtained. The response surface plot is a graphical representation of Eq. (6). As can be seen, the response surface is pseudo-convex in shape. From this Figure, it can be stated that the total removal of tartrazine can be achieved within a wide interval of operational conditions. Hence, it is of the utmost importance to determine the optimal operating conditions that maximize tartrazine removal. Table 3 summarizes the coded and real values of the operational variables that, at least theoretically, lead to a maximization of the removal efficiency. It is worth noting that the optimal experimental conditions are in the close vicinity of the central point (0, 0) of the experimental design (namely, 0.0353, 0.0313). This is indicative of an adequate selection of the working interval.

3.1.2. Study of the TOC removal as the target variable

The percentage of TOC removed is commonly accepted as an indicator of the degree of mineralization achieved by an advanced oxidation process. Therefore, it has been considered appropriate to analyze the efficiency of TOC removal as the second target variable in this work. Indeed, the degree of mineralization achieved is as important as -or even more than-a high percentage of pollutant removal. This is so because, as is well known, some intermediate by-products of advanced oxidation processes can exhibit the same or even greater toxicity than the pollutant initially present in the water. The analysis of the statistical design of experiments is much the same as for dye removal efficiency and, thus, it will be discussed in a less detailed manner in this section. Table S1 (Supplementary Material) also lists the results of the ANOVA test for the TOC removal efficiency. From the results of the p-value it can be concluded that, in this case, both operating variables exert a statistically significant influence on the target variable, as does the quadratic term of current density. This is corroborated from the Pareto plot shown in Fig. S2, top (Supplementary Material). Fig. S2, bottom (Supplementary Material) illustrates the influence of current density and initial concentration of tartrazine on the TOC removal efficiency. As it was the case for dye removal, the TOC removal efficiency increases as current density does until a maximum is achieved. Such an increase is attributable to the concomitant generation of larger amounts of HO· radicals on the BDD as indicated by Eq. (1). However, once a given value of j is reached, only a slight increase in TOC removal percent can be observed, despite the larger amount of hydroxyl radicals that are generated on the surface of the BDD electrode. This latter may be due to the occurrence of parallel parasitic reactions such as the so-called *oxygen evolution reaction* at the anode, Eq. (7), or the dimerization reaction of hydroxyl radicals to yield hydrogen peroxide, Eq. (8):

$$2BDD(HO\cdot) \longrightarrow 2BDD + O_2 + 2H^+ + 2e^- \quad (7)$$

$$2BDD(HO\cdot) \longrightarrow 2BDD + H_2O_2 \quad (8)$$

As a consequence of these reactions, a decreased availability of HO· radicals at the anode results in a decrease in TOC removal efficiency (and, probably, dye removal efficiency, too). To sum up, as j increases, larger amounts of BDD(HO·) are consumed in non-oxidizing reactions, thus decreasing the overall efficiency of the electro-oxidation process. This behavior has been repeatedly described previously in the literature (Barisci and Suri, 2020; Zhu et al., 2019; Wachter et al., 2019; Vasconcelos et al., 2019; Valenzuela et al., 2017; Salazar et al., 2016). Unlike in the case of tartrazine removal efficiency, the initial concentration of dye exerts a positive, although not very marked, effect on TOC removal efficiency. This latter is in good agreement with the occurrence of a process mostly controlled by mass transport and with a very limited contribution of mediated oxidation (Martin de Vidales et al., 2012). In other words, the electro-oxidation process is mainly governed by the mass transfer rate of the pollutant from the bulk solution towards the anode's surface (Oturan et al., 2011). Another plausible explanation could be that if higher concentrations of pollutants are found in solution, HO· radicals are preferably consumed in reactions with tartrazine (or

Table 3
Optimal coded and real values for the electro-oxidation processes.

Tartrazine removal efficiency		
Factor	Coded optimum	Real optimum
j (mA ·cm^{-2})	0.0353	34.8
C (mg ·L^{-1})	0.0313	28.6
TOC removal efficiency		
Factor	Coded optimum	Real optimum
j (mA ·cm^{-2})	0.5478	46.3
C (mg ·L^{-1})	1.3788	52.38
Tartrazine removal rate		
Factor	Coded optimum	Real optimum
j (mA ·cm^{-2})	1.3307	62.34
C (mg ·L^{-1})	−0.6508	16.49

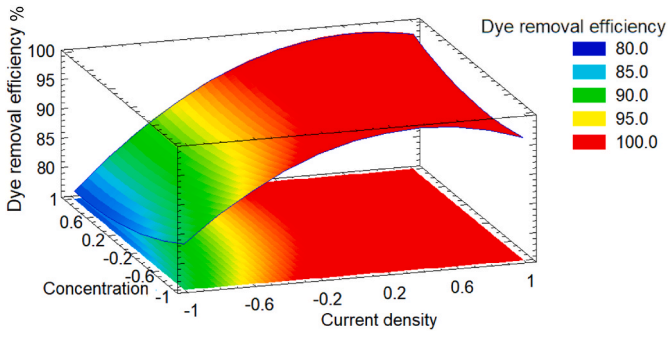

Fig. 3. Response surface plot for the removal efficiency of tartrazine by electro-oxidation with BDD electrodes.

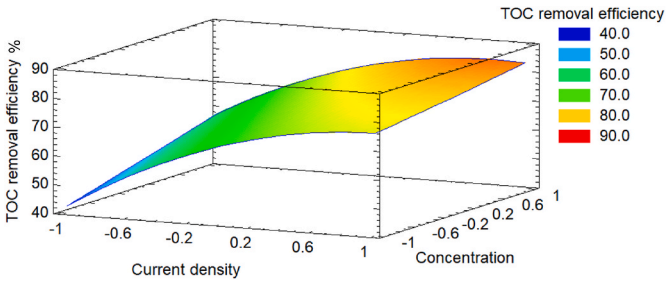

Fig. 4. Response surface plot for the TOC removal efficiency by electro-oxidation with BDD electrodes.

by-products of its degradation), thus decreasing the incidence of the O_2 evolution reaction or the generation of H_2O_2 (Murugananthan et al., 2008; He et al., 2015). The regression equation that correlates TOC removal efficiency with the operational variables, j and C, is:

$$TOC\ removal\ efficiency\ (\%) = 72.884 + 14.6058 \cdot j + 5.95408 \cdot C - -8.11082 \cdot j^2 - 1.88 \cdot j \cdot C + 0.189184 \cdot C^2 \quad (9)$$

This, again, is in good agreement with the information drawn from the Pareto and main effects plots (Fig. S.2, Supplementary Material). According to all the above exposed it becomes evident that an adequate selection of the operating conditions is extremely important. The response surface plot for the TOC removal efficiency is depicted in Fig. 4. Form this Figure, it can be clearly appreciated that the maximum TOC removal efficiency is around 85–90% and it can be achieved in the upper-right corner of the surface plot. Taking this into consideration, an optimum has been found for the TOC removal by electro-oxidation with BDD electrodes. The experimental conditions that lead to an optimum in the mineralization degree are also summarized in Table 3. At least theoretically, operating under these experimental conditions a mineralization degree of up to 85.6% can be achieved.

3.1.3. Study of the tartrazine removal rate as the target variable

In order to analyze the removal rate of the pollutant, a series of preliminary tests were performed to determine the order of the kinetic process. The C vs. t plots for the removal efficiency of tartrazine at different initial concentrations by electro-oxidation with BDD electrodes are shown in Fig. S3 (Supplementary Material). The experimental data were fitted to the pseudo-first and pseudo-second kinetic models. Although both models can fit reasonably well the experimental data, the best results were obtained by applying the pseudo-first order model. The rate constants corresponding to each of the 16 experiments that constitute the experimental matrix of the statistical design are listed in Table 1. The results of the ANOVA test are listed in Table S1 (Supplementary Material). Both, the current density and the initial concentration of tartrazine, as well as the squared term of the later, exert a significant effect on the kinetic rate of tartrazine degradation. This, again, is corroborated by the Pareto plot depicted in Fig. S4, top (Supplementary Material). Fig. S4, bottom, depicts the main effect plot for the tartrazine removal rate. The positive influence of the current density on the removal rate constant shown in this Figure is compatible with the fact that increasing current density increases the overpotential, which, in turn, results in the formation of larger amounts of electro-generated HO· radicals in shorter times. Hence, these radicals are readily available for dye degradation (Punturat and Huang, 2016). Moreover, the presence of sulfate as the supporting electrolyte also plays an important role in the removal rate of tartrazine and its effect cannot be neglected. In fact, when sulfate anions migrate to the BDD anode $SO_4^{\cdot-}$ radicals are formed on the surface of the electrode, where uncatalyzed oxidation of SO_2^{2-} or HSO_4^- takes place at lower potentials than oxygen evolution from water oxidation (Davis et al., 2014). Sulfate radical species ($SO_4^{\cdot-}$ or $HSO_4^{\cdot}$) may be produced either by direct electron transfer on the surface of the BDD anode or by the reaction of sulfate anions with hydroxyl radicals.

As the current density increases, the generation of sulfate radicals does as well. Sulfate radicals themselves may act as oxidizing agents (Farhat et al., 2015; Davis et al., 2014). Moreover, sulfate radicals may recombine with each other, thus leading to the formation of persulfate ions, a powerful oxidizing agent as well. This contributes to higher electro-oxidation rates of the target pollutant. To sum up, large values of current density favor the generation of mediated electro-reagents on the surface of the electrode thus giving rise to faster degradation of tartrazine.

From the main effects plot it can be also stated that the initial concentration of pollutant exerts a less remarkable influence on the removal rate of tartrazine. At low values of initial pollutant concentration, as C increases the removal rate constant remains almost unchanged or increases very slightly. However, from a given value of initial concentration, a further increase in this variable results in a decrease in the removal rate constant. It must be taken into account that the increase in tartrazine concentration results in an increased concentration gradient. Hence, the mass transfer of the pollutant towards the anode surface is favored. If $j < j_{lim}$ -which is the case-the electrolysis process is controlled by mass transfer phenomena and the removal rate constant should increase. However, as the initial concentration increases, the oxidation of larger amounts of the target compound -and its degradation intermediates as well-progressively require more hydroxyl radicals. This, in turn, results in the decrease in tartrazine removal rate as depicted in Fig. S4 bottom (Supplementary Material).

As in the preceding subsections, a regression equation that correlates the tartrazine removal rate with the operational variables, j and C, has been proposed:

$$Removal\ rate\ constant\ (min^{-1}) = 0.0830255 + 0.0378014 \cdot j - 0.012618 \cdot C - -0.00592616 \cdot j^2 + 0.006425 \cdot j \cdot C - 0.00895207 \cdot C^2 \quad (10)$$

From the relative values of the correlation coefficients, it may be concluded that -as suggested by the Pareto plot and the ANOVA test- current density is the main factor governing the removal rate of tartrazine, followed by initial concentration and, to a lesser extent, by the squared term of C.

Again, it can be stated that an adequate selection of the operating conditions is very important to ensure the fastest removal of tartrazine.

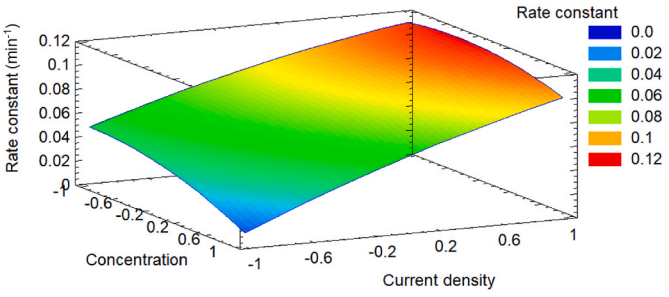

Fig. 5. Response surface plot for the tartrazine removal rate constant by electro-oxidation with BDD electrodes.

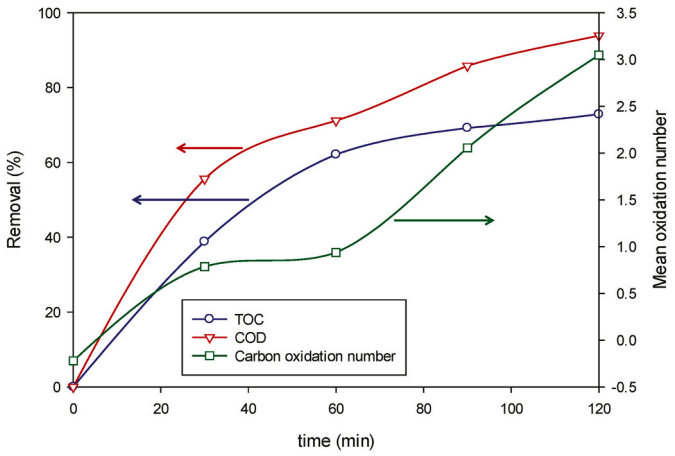

Fig. 6. Temporal evolution of COD and TOC removal (left Y-axis) and MOC (right Y-axis) for the tartrazine removal by electro-oxidation with BDD electrodes.

Obviously, the faster the electro-oxidation process takes place, the shorter operational times are required which may yield a remarkable decrease in the operational costs. The response surface plot for the removal rate constant is depicted in Fig. 5. Form this Figure, it can be appreciated that, operating under the experimental conditions located at the upper right corner of the response surface plot, a maximum in tartrazine removal rate can be achieved. Such a theoretical optimum corresponds to the operational conditions summarized in Table 3. At least theoretically, operating under these experimental conditions, a removal rate constant of up to 0.1217 min^{-1} can be achieved.

3.1.4. Temporal evolution of TOC and COD, and mean oxidation number of carbon

To analyze COD and TOC evolution with time, the central coded experiment (0,0) was monitored as depicted in Fig. 6. This Figure points out that tartrazine mineralization by electro-oxidation processes is feasible and takes place in a fast manner. It can be stated that COD removal takes place to a greater extent than TOC removal does, regardless of what the reaction time is. Starting from initial values of COD and TOC of 36 mg $\cdot L^{-1}$ and 12.8 mg $\cdot L^{-1}$, respectively, removals efficiencies of up to 94.4% and 72.8% of COD and TOC, respectively, are obtained. This suggests that the organic matter initially present in water is mineralized to a large extent.

One of the main advantages of the advanced oxidation processes, in general, and electrochemical oxidation processes, in particular, is the fact that, at least theoretically, the pollutant(s) initially present in the solution can be oxidized until total mineralization is achieved and the final products of the process are carbon dioxide and water.

In order to check the evolution of the mineralization degree with time, the so-called *mean oxidation number of carbon* (MOC) has been proposed (Vogel et al., 2000). Briefly, when the composition of the wastewater is known - as it is the case in this work - the analysis of the MOC values provide valuable information on the progress of the electro-oxidation process. According to Vogel et al. (2000) MOC can be calculated as:

$$MOC = 4 - 1.5\frac{COD}{TOC} \quad (11)$$

From Fig. 6 it can be observed that the mean oxidation carbon value of the initial tartrazine solution (i.e., the one determined at t = 0 min) is approximately −0.22. This value is coherent with the presence in the tartrazine molecule of carbon atoms that are mainly included in aromatic rings and carboxylate groups. As the tartrazine electro-oxidation process evolves, the MOC value increases progressively. Thus, at treatment times of 30 and 60 min, MOC reaches values of 0.8–0.9, which are compatible with short-chain dicarboxylic acids as, for instance, maleic acid. At longer treatment times (90 min) MOC is approximately equal to +2, i.e., the value corresponding to formic acid. Finally, for treatment time equal to 120 min, the value of MOC is +3, a value that corresponds to oxalic acid. This latter compound is on the step immediately preceding the complete mineralization of organic carbon into carbon dioxide.

Although the MOC is a useful tool to monitor the evolution of the mineralization of tartrazine by electro-oxidation with BDD electrodes, it must be taken into consideration the presence of an azo (-N=N-) group in the chemical structure of the dye that may undergo oxidation from the oxidation number of −1 up to dinitrogen molecule (with oxidation number equal to zero). Hence, the MOC value determined according to equation (11) will be lower since not only carbon but also nitrogen undergoes oxidation. The same applies to the presence of sulfur in the form of sulfonic groups (oxidation number = +4) that are oxidized to SO_3 (oxidation number = +6) thus giving rise, again, to an underestimation of the MOC value.

Consequently, the actual average oxidation number of carbon will be even higher than +3, and the mineralization of tartrazine by electro-oxidation may be regarded as almost complete. Hence, it can be stated that electro-oxidation of tartrazine with BDD electrodes is an adequate method to achieve complete and fast removal of this pollutant from water, as well as almost complete mineralization of the dye and its intermediate byproducts.

3.1.5. Experimental confirmation of the theoretical optimum

In order to corroborate that the experimental conditions predicted by the model are suitable for the removal of tartrazine in aqueous solution, experiments were conducted under such optimal conditions. Operating under the theoretical conditions predicted by the model when the target variable is dye removal (see Table 3) up to 99.6% removal efficiency was obtained. Similarly, when performing an experiment under the theoretical conditions that lead to the simultaneous optimization of the removal efficiency and the specific rate constant "k" (Table 3) the removal efficiency was 98.8% and the specific rate constant was 0.082 min^{-1}.

According to these experimental results, it is possible to state, firstly, that the proposed theoretical model can predict the experimental results very satisfactorily. Secondly, it is possible to remove virtually all of the dye initially present in the solution by operating under the appropriate conditions and to do so in a short time, which in turn results in a reduction in operating costs.

3.2. Sonochemical oxidation process

As indicated above, the technical limitations of the ultrasound equipment made it impossible to perform a statistical design of experiments to analyze the influence of different operational parameters on the sonochemical degradation of tartrazine. Nevertheless, a set of 8 experiments were carried out and the experimental results are listed in Table 2. In the following sections, the influence of three operational parameters such as power, frequency, and pulse-stop ratio is discussed to some extent.

3.2.1. Influence of ultrasound power

The ultrasound power (or amplitude) affects the phenomenon of acoustic cavitation and, as a consequence, exerts a noticeable influence on the sonochemical reactions. From the results listed in Table 2, it can be concluded that an increase in the ultrasound power from 2.0 up to 10.9 W $\cdot L^{-1}$ results in an increase of removal efficiency from 6.0 up to 28.2% (i.e., 4.7 times larger). On the contrary, a further increase of this parameter reaching 26.6 W $\cdot L^{-1}$ is coupled to a very modest improvement of the removal efficiency (28.2–31.4%). According to the literature, for the different sonochemical oxidation processes, a threshold value of intensity can be determined. Below such a value, the

sonochemical oxidation barely occurs, since cavitation takes place to a very limited extent (Tran et al., 2015). From this value on, sonochemical oxidation is progressively more efficient as ultrasound power rises until a maximum is attained. Probably, an increase in ultrasound power leads to a higher rate of H_2O_2 molecules breakage in aqueous solution. As a consequence, the concentration of HO· radicals increases, and the radical-mediated degradation of the organic molecules of the pollutant is more likely to take place (Guo et al., 2010). Furthermore, as ultrasonic power rises, the mixing efficiency is improved, since turbulence and microstreaming are generated as a consequence of the cavitational collapse of microbubbles (Lianou et al., 2018; Asgari et al., 2020).

However, once the upper limit is reached, a further increase in ultrasound power results in a very limited improvement of the removal efficiency. A plausible explanation to this fact is that, at high values of ultrasound power, a coalescence of the ultrasound-generated bubbles may occur, thus giving rise to an increase in their size. This, in turn, leads to lower pressure pulses when the bubbles eventually collapse.

According to the results summarized in Table 2, this appears to be the case for the sonochemical oxidation of tartrazine. Hence, an ultrasound power equal to 10.9 $W{\cdot}L^{-1}$ was selected for the subsequent experiments, since an increase of the power up to 26.6 W $\cdot L^{-1}$ does not lead to a remarkable improvement in removal efficiency but leads to much higher operational costs.

3.2.2. *Influence of ultrasound frequency*

The ultrasound frequency applied in sonochemical oxidation is a very important parameter since it conditions the generation of both, micro-bubbles and HO· radicals during the acoustic cavitation (Sathishkumar et al., 2016). Hence, further experiments were performed keeping the ultrasound power fixed at 10.9 $W{\cdot}L^{-1}$ and varying the ultrasound frequency.

From the results summarized in Table 2, it can be concluded that, as the ultrasound frequency increases from 578 up to 1140 kHz the removal efficiency of tartrazine remains constant (18.0–19.4%). Similar results were recently reported by Kidak and Dogan (2018), and Vega et al. (2019) for the removal of amoxicillin and triclosan, respectively. Nevertheless, according to the literature, the application of low-frequency ultrasound (e.g., 20 kHz) with sonochemical oxidation purposes generates a lower number of active bubbles than those strictly required for the sonochemical reactions to take place (Sathishkumar et al., 2016). However, if the frequency remains relatively low but reaches a minimum value, the bubbles generated under have more time to increase in diameter, thus reaching a larger maximum size. Such bubbles collapse more violently releasing a higher concentration of HO· radicals with strong oxidizing potential. This, in turn, makes the extent of degradation increase. On the contrary, if high ultrasound frequency is applied (e.g., above 1 MHz) a lower amount of active radicals is generated, probably because high-frequency bubbles have a small maximum diameter and hence release less energy. Although the collapse of generated bubbles is faster and more violent at high frequencies, thus increasing the pressure generated, the efficiency in the HO· radicals generation is increased until an optimal value is reached (Hung and Hoffmann, 1999; Gogate et al., 2003). Above this optimal frequency, the effect of cavitation is reduced, as indicated above.

Another plausible explanation to this controversial effect of frequency is that, due to wave refraction, at high values of frequency a negative pressure in the bulk solution is generated or the prevalence of bubbles is insufficient (Thompson and Doraiswamy, 1999; Quesada-Penate et al., 2009; Dukkanci et al., 2012). On the contrary, if low ultrasound frequency is used, the production of active bubbles is handicapped due to the presence of a relatively higher amount of water vapor inside the collapsing bubbles. Under the optimal conditions, a large number of active bubbles and radicals are generated during the acoustic cavitation (Findik et al., 2006).

The experimental results obtained in this work suggest that the use of frequencies above 578 kHz does not lead to higher removal rates but result in higher operational costs. Hence, 578 kHz was fixed as the treatment frequency for subsequent experiments.

3.2.3. *Influence of the pulse-stop ratio*

Taking the previous experimental results as the starting point, an optimal frequency of 578 kHz was selected to analyze the influence of the pulse-stop (p-s) time, on the removal efficiency of tartrazine. Also, ultrasound power was fixed at its optimum value, 10.9 $W{\cdot}L^{-1}$. From the experimental results (see Table 2) it can be stated that the highest tartrazine removal efficiencies were obtained using p-s values of 250-50 ms and 100-50 ms, corresponding to p-s ratios equal to 5:1 and 2:1. The use of a lower p-s ratio (as 1:1) was detrimental to pollutant's removal.

The effect of pulsed ultrasound on sonochemical oxidation is less known in comparison with that of power and frequency. In pulsed radiation, ultrasound is emitted in intermittent pulses of specific duration. If pulsed ultrasound radiation is properly applied, diffusion of the molecules to the bubble interface -where the reaction is taking place-is enhanced. Furthermore, diffusion to the cavitation bubbles is favored for small molecules, particularly those with molar volumes below 130 mL $\cdot mol^{-1}$. Since the molar volume of tartrazine, estimated as proposed by Fedors (1974) is approximately 155 mL $\cdot mol^{-1}$, it can be assumed that tartrazine can diffuse reasonably well to the bubble interface and its degradation is favored by applying pulsed ultrasound radiation.

The use of pulsed ultrasound gives rise to *transient cavitation* that is highly efficient in generating chemical reactions (Henglein et al., 1989). When the bubbles formed by transient cavitation undergo implosion, high temperature is reached, high pressure is generated and large amounts of strongly oxidizing free radicals (e.g., HO·) are produced. However, if the duration of the intermittent pulse of sonication is short in comparison with the pause period, oscillation and implosion of transient bubbles either do not take place or occur to a very limited extent. Hence, most of the ultrasound-generated bubbles remain unaltered when the ultrasound pulse stops. Next, during the pause period, the pressure generated by the ultrasound radiation ceases and the bubbles relax. As a result, when the next pulse of ultrasound radiation is applied, much greater pressure is required to cause the bubbles to implode. Because of this decrease in bubble implosion, if the radiation pulse is too short compared to the pause period, less free radicals are generated, and the ability to degrade the contaminant by using pulsed ultrasound radiation is lower than if continuous radiation is used (Thompson and Doraiswamy, 1999). This is coherent with the low degradation efficiency of tartrazine obtained using a pulse-stop ratio

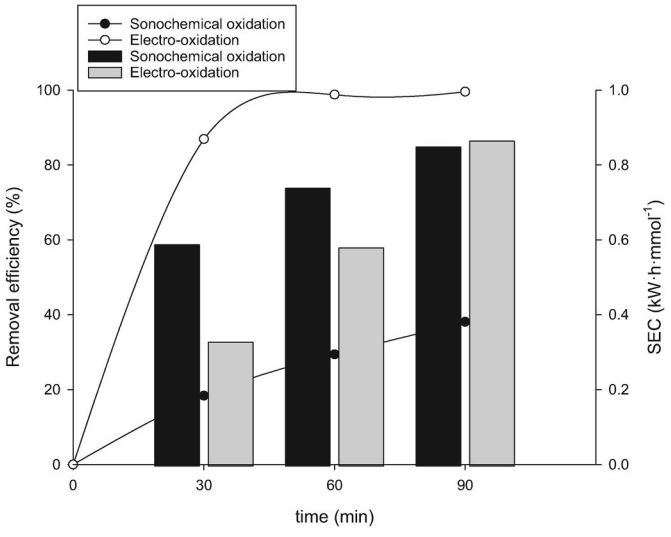

Fig. 7. Comparison of kinetics (lines and dots plots, left Y-axis) and energy consumption (bars charts, right Y-axis) for both processes, electrochemical oxidation and ultrasound oxidation.

equal to 1:1 (i.e., 100 ms pulse followed by 100 ms stop). On the contrary, if larger pulse-stop ratios are used large amounts of bubbles are formed through transient cavitation, which results in higher removal efficiencies for pulse-stop ratios of 250-50 ms (5:1) or 100-50 ms (2:1). Taking into account energy and economic considerations, a pulse-stop ratio equal to 2:1 (i.e., 100-50 ms) appears as the best option for the sonochemical oxidation of tartrazine.

3.3. Electrochemical versus sonochemical process. Kinetic and energetic comparison

In this section, relevant aspects of both processes will be compared from the kinetic and energetic standpoints, in order to estimate the operating costs.

Fig. 7 depicts the variation of the removal efficiency of the target pollutant with time (dots and line plots) throughout an electro-oxidation experiment (namely, a central experiment with coded values of j and C equal to zero), and one sonochemical oxidation experiment (the one performed under optimal conditions). From this plot, it can be easily deduced that the electrochemical process is approximately three times faster than the sonochemical one. Furthermore, as indicated previously, the electrochemical process is clearly more efficient in terms of pollutant removal.

Nevertheless, in order to compare the efficiency of both types of processes in terms of energy consumption, the Specific Energy Consumption (SEC) parameter can be defined as follows:

$$SEC = \frac{w \cdot t}{V \cdot (C_0 - C_t)} \quad (12)$$

where w is the power (in W); t is the reaction time (in hours); C_0 and C_t are the pollutant concentration (in mM) at the beginning of the experiment and after a time, t, is elapsed, respectively; and V is the volume of solution (in L). It is worth noting that, for the electrooxidation process, the power was calculated as the product of potential (in volts) and the intensity (in amperes), whereas for the sonochemical method, energy data were measured directly in the solution by a calorimetry method previously described in the literature (Koda et al., 2003).

The SEC vs time data are also depicted (column plots) in Fig. 7. As can be seen in this Figure, the energy costs are, as a rule, competitive in both cases. However, the experimental results clearly indicate that for short or intermediate reaction times (i.e., 30 or 60 min of treatment) the electro-oxidation process seems to be advantageous from the standpoint of energy consumption per mmol of dye removed. Nevertheless, if longer reaction times are used (i.e., 90 min) the specific energy consumption per mmol of tartrazine is much the same, regardless of the type of treatment chosen.

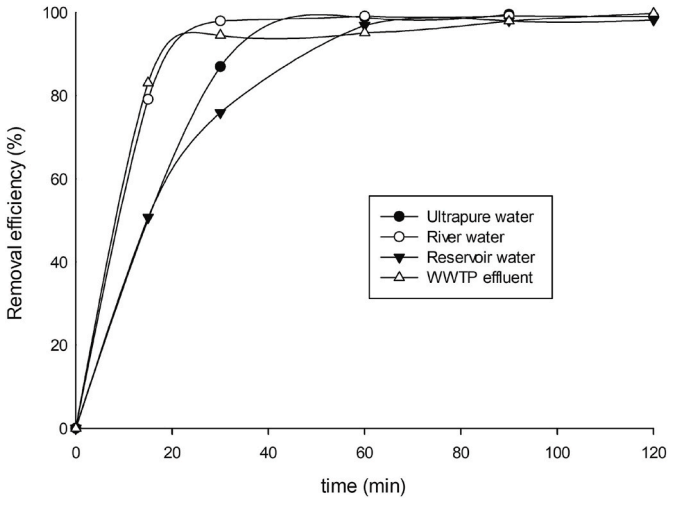

Fig. 8. Influence of the aqueous matrix on the electrochemical oxidation process.

3.4. Influence of the aqueous matrix on the electro-oxidation process

In order to analyze the influence of the aqueous matrix on the removal of tartrazine from water, three different aqueous matrices, namely from a reservoir, the Guadiana river, and an effluent from a local wastewater treatment plant were used. The main physical and chemical parameters of the different water matrices are summarized in Table S2 (Supplementary Material).

In all the electro-oxidation experiments, the removal of tartrazine was determined at 15, 30, 60, 90, and 120 min of treatment, whereas the TOC and COD removal were determined at the end of the treatment time. The experimental results are depicted in Fig. 8. From this Figure, it can be stated that the total removal of tartrazine can be achieved after 120 min of electrochemical treatment in all the aqueous matrices. However, noticeable differences can be observed between them in terms of kinetics. In order to discuss such differences, the physical and chemical properties of the aqueous matrices listed in Table S2 (Supplementary Material) must be taken into consideration. Also, for the sake of comparison, the parameter t_{90} (i.e., the time required to achieve 90% of tartrazine removal) can be of much help. The values of t_{90} for ultrapure, river and reservoir water, and WWTP effluent are 32, 19, 47, and 17 min, respectively. From the shape of the removal efficiency vs. time depicted in Fig. 8, as well as from the values of t_{90}, it can be easily deduced that the removal of tartrazine is faster in river water and WWTP effluent than in ultrapure water. On the contrary, larger time is needed to reach 90% removal efficiency in reservoir water.

The most feasible explanation to this fact is that the removal rate depends mainly on two factors: on the one hand, the nature and concentration of ions; and, on the other hand, the presence of organic matter in the aqueous environment. It is well-known that the presence of large concentrations of ions (mainly chloride and/or nitrate) in the aqueous matrix may result in the formation of different radical species that can also contribute to degrading the target pollutant. This positive effect of the presence of nitrate and chloride ions has been previously reported when similar aqueous matrices were used to study the electro-oxidation process of parabens Dominguez et al. (2016). On the contrary, the presence of high contents of organic matter in the medium would hamper the oxidation process, since a portion of the electro-generated hydroxyl radicals would be consumed in the degradation of the organic matter so that it would not be available for the removal of tartrazine.

Taking this latter into account, it is worth noting that the degradation of tartrazine in reservoir water is slower than in river water. Although both aqueous matrices exhibit similar organic matter contents, the total ions concentration in reservoir water is lower, as pointed out by the electric conductivity of both water samples (namely, 487 vs. 107 $\mu S \cdot cm^{-1}$ for river and reservoir water, respectively). Also, the degradation rate of tartrazine in reservoir water is somewhat lower than in ultrapure water. Hence, it may be concluded that the positive effect attributable to the presence of ions in reservoir water cannot compensate for the negative effect caused by the organic matter content.

Finally, Fig. S5 (Supplementary Material) shows the efficiency of TOC and COD removal after 120 min of electrooxidation treatment of the different aqueous matrices. It can be easily seen that the sample with the highest ion content (i.e. WWTP effluent) achieves almost complete COD removal (97.68%) but a relatively low degree of mineralization (32.30% reduction in TOC content). In contrast, TOC and COD removal efficiencies from river and reservoir water are significantly lower, with a degree of mineralization slightly above 20% and a reduction in COD content of 30–35%. Ultrapure water shows almost complete removal of COD (94.4%), and a high degree of mineralization (72.7% TOC reduction).

Perhaps the most remarkable feature in Fig. S5 is that WWTP water

and ultrapure water show similar -and high-values of COD removal (above 94% in both cases) but differ significantly in the degree of mineralization achieved. To explain this behavior, it must be taken into account that the presence of ions and other chemical species in WWTP water (chloride, sulfate, ammonium, carbonate, phosphate, and organic matter, among others) can influence the degradation and mineralization of organic compounds by electrochemical treatment.

The influence of these species will depend on the nature and concentration in which they are found, and can inhibit, promote, or even have neutral effects on the electrochemical performance. In general, a positive influence is related to indirect oxidation mediated by radicals or oxidizing agents that are generated on the surface of the anode and next migrate into the solution.

Based on the Cl^- ion content of the WWTP effluent (2.46 mM; see Table S2 in the Supplementary Material), the electro-generation of chlorine gas at the anode, Eq. (13), is feasible.

$$2Cl^- \longrightarrow Cl_2 + 2e \quad (13)$$

The chlorine gas formed reacts with the aqueous phase undergoing dismutation to regenerate Cl^- ions and give rise to HClO, Eq. (14). The latter (or its dissociated form, the hypochlorite anion) can also behave as a powerful oxidizing agent of organic contaminants. The presence of these species will depend on the pH of the medium, Eq. (15). Thus, HClO is the prevalent species for pH values comprised between 3 and 8, whereas at pH above 8 dissociation into ClO^- is favored (Korbahti and Tasyurek, 2015).

$$Cl_2 + H_2O \longrightarrow HClO + H^+ + Cl^- \quad (14)$$

$$HClO \longrightarrow ClO^- + H^+ \quad (15)$$

A similar effect was observed by Zhao et al. (2014) on the electrochemical degradation of bisphenol A. The presence of NaCl in the medium increased the percentage of COD removal up to 92.2% compared to 23% (approximately) obtained in the absence of NaCl.

With regard to the TOC removal efficiency in both cases, certain aspects must be taken into account, such as the presence of other substances that can interfere with the amount of chlorine species present in the medium, and the amount of electro-generated hydroxyl radicals on the surface of the anode. The test performed in ultrapure water has shown that the electrooxidation treatment is effective for the complete elimination and reduction of TOC, and that it is further enhanced by the presence of chloride ions in the medium.

However, as the treatment time elapses, the content of chlorine-mediated species is reduced. Furthermore, these substances will contribute not only to the degradation of the azoic dye, but also to the reduction of organic matter present in the wastewater as well as to the oxidation of other natural components. Zollig et al. (2017) studied the degradation of ammonia and the reduction of COD content of urine samples by electrolysis using a BDD electrode as the anode. They observed that the oxidation of NH_3 to NO_3^- was mediated by the presence of chloride, so that the direct oxidation of NH_3 on the electrode surface and by hydroxyl radicals was negligible. Panizza and Martinez-Huitle (2013) applied electrochemical oxidation to treat a landfill leachate using different materials as the anode ($TiRuSnO_2$, PbO_2, and BDD). The results obtained with the BDD anode indicated a complete reduction in COD and ammonia contents. This effect was related to the high concentration of Cl^- present in the effluent to be treated which would lead to the generation of active chlorine during electrooxidation, Eq. (13), and HClO, Eq. (14), which would react with the NH_4^+ present by means of "breakthrough reactions". Therefore, the presence of NH_4^+ in the medium plays an important role in the electrooxidation treatment, since part of the reactive chlorine species could be used to oxidize NH_4^+ to its maximum oxidation state, NO_3^-. To sum up, part of the chlorinated oxidants would be used to degrade the dye, part to remove some of the natural organic matter from the water, and part to oxidize the NH_4^+ to NO_3^-. Nitrate has been used as an inert electrolyte in electrochemical oxidation processes to evaluate the direct oxidation of organic contaminants by HO· radicals (Jardak et al., 2016). Indeed, these species would not contribute to the degradation and mineralization of the compound, and the presence of NH_4^+ would exert a negative effect. On the other hand, the simultaneous presence of NO_2^- and NO_3^- can lead to the formation of NH_3, Eqs. (16)–(18).

$$NO_3^- + 6H_2O + 8e \longrightarrow NH_3 + 9OH^- \quad (16)$$

$$NO_3^- + H^+ + 2e \longrightarrow NO_2^- + H_2O \quad (17)$$

$$NO_2^- + 5H_2O + 6e \longrightarrow NH_3 + 7OH^- \quad (18)$$

Ammonia, in turn, can compete with tartrazine for HO· radicals, Eq. (19) (Wang et al., 2019).

$$NH_3 + 6HO\cdot \longrightarrow N_2 + 5H_2O + 6e \quad (19)$$

The organic matter content in real aqueous matrices is also a factor that can affect the efficiency of the electrochemical treatment. Some of this organic matter is often dissolved in the form of humic acids (HA), which are high molecular weight compounds. The presence of HA negatively affects the oxidation process by competing with tartrazine for reactive species and electrode surface sites, thus leading to lower degradation efficiencies as the concentration of HA increases. This effect was studied by Woisetschlager et al. (2013) when treating synthetic solutions containing glucose and HA. Therefore, a real water matrix with a high organic matter content can decrease the efficiency of the process since lesser amounts of HO· radicals would be available to degrade the target compound.

Another factor to be taken into account in the electrooxidation treatment is the concentration of HO· radicals, since the degradation depends largely on the amount of these radicals generated in the process. The pH is a parameter that affects the rate of formation of the HO· radical, so that higher concentrations of this species are generated in acidic pH. Moreover, it must be taken into account that the redox potential of this species is dependent on the pH value of the medium, the potential being higher in acidic conditions (2.85 V) than under alkaline conditions (2.02 V) Zhao et al. (2014). The pH conditions in the water matrices used in this work were slightly alkaline (see Table S.2 of the Supplementary Material). On the contrary, the tests in UP water were performed at the pH of the tartrazine solution. Such a pH was initially equal to 7.8, although it decreased steadily with the reaction time, thus reaching acidic conditions. The higher concentration of HO· radicals, as well as the higher oxidation potential under these conditions, would influence the TOC removal rate in a positive manner.

With respect to the COD removal, similar values were obtained in both matrices (UP water and WWTP effluent), although the amount of COD removed in the WWTP water was slightly higher. The presence of chloride ions allowed the almost complete oxidation of tartrazine and other constituents initially present in the effluent. This study has shown that tartrazine is easily degradable and oxidizable by electrooxidation, so the presence of chloride in WWTP effluent would counteract the negative effects related to pH, presence of other ions (such as ammonium, nitrate, or nitrite, among others) and organic matter. In fact, for aqueous matrices with a lower Cl^- content but similar pH and organic matter contents (river and reservoir water), lower percentages of COD removal were obtained (approximately 35%) compared to 97.68 and 94.4% obtained in WWTP effluent and UP water respectively. This latter demonstrates the importance of the presence of chloride ions, and the absence of organic matter, in the reduction of the COD for WWTP effluent and UP water, respectively.

Finally, in relation to the residual TOC content after the electrooxidation treatment, the results indicate remarkable differences between the real water matrices and the tests carried out in UP water. The reduction in TOC content is slower than the oxidation of organic matter,

since it requires the conversion of non-oxidizable substances, such as formic acid or oxalic acid, into CO_2 and water. These by-products are, hence, recalcitrant compounds that could resist oxidation by HO· radicals and therefore would require longer treatment times. The high organic matter content in the real water matrix would lead to the presence of less HO· radicals available to mineralize the target compound. In addition, the organic matter would minimize the number of active sites on the surface of the anode. The results of COD and TOC removal in ultra pure water (94.4 and 72.7%, respectively) clearly indicate that most of the by-products present after the electrooxidation process would be short-chain carboxylic acids, which, as mentioned above, are difficult to degrade.

4. Conclusions

From the results obtained in the present study the following conclusions may be drawn:

- The BDD electrochemical oxidation makes it possible to achieve the total removal of tartrazine in ultrapure water. The main factor governing the process is the current density (*j*). This factor positively influences the removal efficiency of pollutant until a maximum is attained. From this optimal value, a further increase in *j* results in a rapid decrease in the removal efficiency. The initial concentration of tartrazine exerts a much more limited effect on the removal efficiency.
- The percentage of TOC removed in ultrapure water follows a very similar behavior to that shown by the tartrazine removal efficiency. The occurrence of parallel parasitic reactions (namely, oxygen evolution reaction or hydroxyl radical recombination to yield hydrogen peroxide) clearly hinders the TOC removal.
- The removal rate of tartrazine in ultrapure water is also mainly governed by the current density. However, as expected, in this case, the initial concentration of pollutant also exerts a statistically significant influence.
- The temporal evolution of TOC, COD, and MOC has been analyzed as well. The experimental results point out that, at the end of the electro-oxidation process, a remarkable mineralization of the pollutant has been achieved. Furthermore, the value of MOC is -at least theoretically-equal to +3, although underestimation of this value due to the presence of azo and sulfonic groups in the molecule of tartrazine cannot be discarded.
- The sonochemical oxidation of tartrazine has also been studied. Although, as a rule, lower removal efficiencies of the pollutant are achieved, if ultrasound power and frequency, as well as pulse-stop ratio, are carefully controlled, the sonochemical process can be regarded as an adequate complement to the BDD electro-oxidation of tartrazine.
- The electrochemical and sonochemical processes have been compared in terms of kinetics and energy consumption. It can be stated that, for short treatment times, the electro-oxidation process is advantageous from the energy consumption standpoint. At intermediate treatment times, the operational costs of both processes per mmol of tartrazine removed are much the same. However, at longer treatment times, the ultrasound treatment achieves a more efficient removal of the pollutant in terms of energy consumption.
- Finally, the influence of the aqueous matrix on the removal efficiency of tartrazine was analyzed. It can be concluded that the occurrence of chloride and/or nitrate ions initially present in the aqueous matrices strongly affects the removal efficiency of tartrazine, the decrease in the chemical oxygen demand, and the mineralization degree. All these factors are remarkably influenced by the generation of highly oxidizing radical species from the aforesaid ions, and its concomitant synergistic effect on the removal efficiency of TOC, COD, and target pollutant.

Author contribution statement

G. Donoso: Investigation, Validation. **J.R. Dominguez:** Supervision, Conceptualization, Methodology, Writing- Reviewing and Editing, Conceptualization, Methodology. **T. Gonzalez:** Conceptualization, Methodology, Writing- Reviewing and Editing, Conceptualization, Methodology. **S. E. Correia:** Investigation, Conceptualization, Writing-Original draft preparation, Writing- Reviewing and Editing. **E.M. Cuerda Correa:** Supervision, Conceptualization, Validation, Writing-Original draft preparation, Writing- Reviewing and Editing.

Declaration of competing interest

The authors declare that they have no known competing financial interests or personal relationships that could have appeared to influence the work reported in this paper.

Acknowledgments

The authors gratefully acknowledge the financial support of this research work through the Comisión Interministerial de Ciencia y Tecnología (CICYT)-CTM 2016-75873-R project-as well as through GR15067 and IB16016 projects by the Junta de Extremadura under and the European Regional Development Fund.

Appendix A. Supplementary data

Supplementary data to this article can be found online at https://doi.org/10.1016/j.envres.2021.111517.

References

Amchova, P., Kotolova, H., Ruda-Kucerova, J., 2015. Health safety issues of synthetic food colorants. Regul. Toxicol. Pharmacol. 73, 914–922.
Asgari, G., Shabanloo, A., Salari, M., Eslami, F., 2020. Sonophotocatalytic treatment of ab113 dye and real textile wastewater using zno/persulfate: modeling by response surface methodology and artificial neural network. Environ. Res. 184 https://doi.org/10.1016/j.envres.2020.109367.
Baluchova, S., Danhel, A., Dejmkova, H., Ostatna, V., Fojta, M., Schwarzova-Peckova, K., 2019. Recent progress in the applications of boron doped diamond electrodes in electroanalysis of organic compounds and biomolecules – a review. Anal. Chim. Acta 1077, 30–66.
Barbosa, A., da Silva, L., de Paula, H., Romualdo, L., Sadoyama, G., Andrade, L., 2018. Combined use of coagulation (m. oleifera) and electrochemical techniques in the treatment of industrial paint wastewater for reuse and/or disposal. Water Res. 145, 153–161.
Barisci, S., Suri, R., 2020. Electrooxidation of short and long chain perfluorocarboxylic acids using boron doped diamond electrodes. Chemosphere 243.
Barrera, H., Roa-Morales, G., Balderas-Hernandez, P., Barrera-Diaz, C., Frontana-Uribe, B., 2019. Catalytic effect of hydrogen peroxide in the electrochemical treatment of phenolic pollutants using a bdd anode. ChemElectroChem 6, 2264–2272.
Bensalah, N., Bedoui, A., 2017. Enhancing the performance of electro-peroxone by incorporation of uv irradiation and bdd anodes. Environ. Technol. 38, 2979–2987.
Cai, J., Zhou, M., Liu, Y., Savall, A., Groenen Serrano, K., 2018. Indirect electrochemical oxidation of 2,4-dichlorophenoxyacetic acid using electrochemically-generated persulfate. Chemosphere 204, 163–169.
Candia-Onfray, C., Espinoza, N., Sabino da Silva, E., Toledo-Neira, C., Espinoza, L., Santander, R., García, V., Salazar, R., 2018. Treatment of winery wastewater by anodic oxidation using bdd electrode. Chemosphere 206, 709–717.
Canizares, P., Paz, R., Saez, C., Rodrigo, M., 2007. Electrochemical oxidation of wastewaters polluted with aromatics and heterocyclic compounds. J. Electrochem. Soc. 154, E165–E171.
Canizares, P., Saez, C., Sanchez-Carretero, A., Rodrigo, M., 2008. Influence of the characteristics of p-si bdd anodes on the efficiency of peroxodiphosphate electrosynthesis process. Electrochem. Commun. 10, 602–606.
Chatel, G., Colmenares, J., 2017. Sonochemistry: from basic principles to innovative applications. Top. Curr. Chem. 375.
Collivignarelli, M., Abba, A., Carnevale Miino, M., Damiani, S., 2019. Treatments for color removal from wastewater: state of the art. J. Environ. Manag. 236, 727–745.
Comninellis, C., 1994. Electrocatalysis in the electrochemical conversion/combustion of organic pollutants for waste water treatment. Electrochim. Acta 39, 1857–1862.
da Silva, S., Navarro, E., Rodrigues, M., Bernardes, A., Pérez-Herranz, V., 2018. The role of the anode material and water matrix in the electrochemical oxidation of norfloxacin. Chemosphere 210, 615–623.

Davis, J., Baygents, J., Farrell, J., 2014. Understanding persulfate production at boron doped diamond film anodes. Electrochim. Acta 150, 68–74.
Dominguez, J., Gonzalez, T., Palo, P., Sanchez-Martin, J., 2010. Electrochemical advanced oxidation of carbamazepine on boron-doped diamond anodes. influence of operating variables. Ind. Eng. Chem. Res. 49, 8353–8359.
Dominguez, J., Munoz-Pena, M., Gonzalez, T., Palo, P., Cuerda-Correa, E., 2016. Parabens abatement from surface waters by electrochemical advanced oxidation with boron doped diamond anodes. Environ. Sci. Pollut. Control Ser. 23, 20315–20330.
Dukkanci, M., Vinatoru, M., Mason, T., 2012. Sonochemical treatment of orange ii using ultrasound at a range of frequencies and powers. J. Adv. Oxid. Technol. 15, 277–283.
Farhat, A., Keller, J., Tait, S., Radjenovic, J., 2015. Removal of persistent organic contaminants by electrochemically activated sulfate. Environ. Sci. Technol. 49, 14326–14333.
Fedors, R., 1974. A method for estimating both the solubility parameters and molar volumes of liquids. Polym. Eng. Sci. 14, 147–154.
Feng, L., van Hullebusch, E., Rodrigo, M., Esposito, G., Oturan, M., 2013. Removal of residual anti-inflammatory and analgesic pharmaceuticals from aqueous systems by electrochemical advanced oxidation processes. a review. Chem. Eng. J. 228, 944–964.
Findik, S., Gunduz, G., Gunduz, E., 2006. Direct sonication of acetic acid in aqueous solutions. Ultrason. Sonochem. 13, 203–207.
Floriano, J., Rosa, E., do Amaral, Q., Zuravski, L., Chaves, P., Machado, M., De Oliveira, L., 2018. Is tartrazine really safe? in silico and ex vivo toxicological studies in human leukocytes: a question of dose. Toxicology Research 7, 1128–1134.
Frontistis, Z., Mantzavinos, D., Meriç, S., 2018. Degradation of antibiotic ampicillin on boron-doped diamond anode using the combined electrochemical oxidation - sodium persulfate process. J. Environ. Manag. 223, 878–887.
Ghasemian, S., Asadishad, B., Omanovic, S., Tufenkji, N., 2017. Electrochemical disinfection of bacteria-laden water using antimony-doped tin-tungsten-oxide electrodes. Water Res. 126, 299–307.
Gicevic, A., Hindija, L., Karacic, A., 2020. Toxicity of Azo Dyes in Pharmaceutical Industry, pp. 581–587.
Gogate, P., 2002. Cavitation: an auxiliary technique in wastewater treatment schemes. Adv. Environ. Res. 6, 335–358. https://doi.org/10.1016/S1093-0191(01)00067-3.
Gogate, P., Mujumdar, S., Pandit, A., 2003. Sonochemical reactors for waste water treatment: comparison using formic acid degradation as a model reaction. Adv. Environ. Res. 7, 283–299.
Gonzalez, T., Dominguez, J., Palo, P., Sanchez-Martin, J., Cuerda-Correa, E., 2011. Development and optimization of the bdd-electrochemical oxidation of the antibiotic trimethoprim in aqueous solution. Desalination 280, 197–202.
Guo, W., Shi, Y., Wang, H., Yang, H., Zhang, G., 2010. Sonochemical decomposition of levofloxacin in aqueous solution. Water Environ. Res. 82, 696–700.
He, Z., Ding, W., Xiao, W., Wu, J., Zhang, C., Fu, D., 2015. Doehlert experimental design applied to electrochemical incineration of methyl green using boron-doped diamond anode. Journal of the Taiwan Institute of Chemical Engineers 56, 160–166.
Henglein, A., Ulrich, R., Lilie, J., 1989. Luminescence and chemical action by pulsed ultrasound. J. Am. Chem. Soc. 111, 1974–1979.
Hung, H.M., Hoffmann, M., 1999. Kinetics and mechanism of the sonolytic degradation of chlorinated hydrocarbons: frequency effects. J. Phys. Chem. 103, 2734–2739.
Hupert, M., Muck, A., Wang, J., Stotter, J., Cvackova, Z., Haymond, S., Show, Y., Swain, G., 2003. Conductive diamond thin-films in electrochemistry. Diam. Relat. Mater. 12, 1940–1949.
Iniesta, J., Michaud, P., Panizza, M., Cerisola, G., Aldaz, A., Comninellis, C., 2001. Electrochemical oxidation of phenol at boron-doped diamond electrode. Electrochim. Acta 46, 3573–3578.
Jagannathan, M., Grieser, F., Ashokkumar, M., 2013. Sonophotocatalytic degradation of paracetamol using tio2 and fe3+. Separ. Purif. Technol. 103, 114–118.
Jardak, K., Dirany, A., Drogui, P., El Khakani, M., 2016. Electrochemical degradation of ethylene glycol in antifreeze liquids using boron doped diamond anode. Separ. Purif. Technol. 168, 215–222. https://doi.org/10.1016/j.seppur.2016.05.046.
Kenova, T., Kornienko, G., Golubtsova, O., Kornienko, V., Maksimov, N., 2018. Electrochemical degradation of mordant blue 13 azo dye using boron-doped diamond and dimensionally stable anodes: influence of experimental parameters and water matrix. Environ. Sci. Pollut. Control Ser. 25, 30425–30440.
Khayyat, L., Essawy, A., Sorour, J., Soffar, A., 2017. Tartrazine induces structural and functional aberrations and genotoxic effects in vivo. PeerJ 2017, 1–14.
Kidak, R., Dogan, ., 2018. Medium-high frequency ultrasound and ozone based advanced oxidation for amoxicillin removal in water. Ultrason. Sonochem. 40, 131–139.
Koda, S., Kimura, T., Kondo, T., Mitome, H., 2003. A standard method to calibrate sonochemical efficiency of an individual reaction system. Ultrason. Sonochem. 10, 149–156.
Korbahti, B., Tasyurek, S., 2015. Electrochemical oxidation of ampicillin antibiotic at boron-doped diamond electrodes and process optimization using response surface methodology. Environ. Sci. Pollut. Control Ser. 22, 3265–3278. https://doi.org/10.1007/s11356-014-3101-7.
Lianou, A., Frontistis, Z., Chatzisymeon, E., Antonopoulou, M., Konstantinou, I., Mantzavinos, D., 2018. Sonochemical oxidation of piroxicam drug: effect of key operating parameters and degradation pathways. J. Chem. Technol. Biotechnol. 93, 28–34.
Marmanis, D., Dermentzis, K., Christoforidis, A., 2016. Design and application of electrochemical processes for decolorization treatment of nylanthrene red dye bearing wastewaters. Journal of Engineering Science and Technology Review 9, 111–115.
Martin de Vidales, M., Saez, C., Canizares, P., Rodrigo, M., 2012. Metoprolol abatement from wastewaters by electrochemical oxidation with boron doped diamond anodes. J. Chem. Technol. Biotechnol. 87, 225–231.
Mousset, E., Pechaud, Y., Oturan, N., Oturan, M., 2019. Charge transfer/mass transport competition in advanced hybrid electrocatalytic wastewater treatment: Development of a new current efficiency relation. Appl. Catal. B Environ. 240, 102–111.
Mpountoukas, P., Pantazaki, A., Kostareli, E., Christodoulou, P., Kareli, D., Poliliou, S., Mourelatos, C., Lambropoulou, V., Lialiaris, T., 2010. Cytogenetic evaluation and dna interaction studies of the food colorants amaranth, erythrosine and tartrazine. Food Chem. Toxicol. 48, 2934–2944.
Murugananthan, M., Yoshihara, S., Rakuma, T., Shirakashi, T., 2008. Mineralization of bisphenol a (bpa) by anodic oxidation with boron-doped diamond (bdd) electrode. J. Hazard Mater. 154, 213–220.
Nakamura, K., Guimarães, L., Magdalena, A., Angelo, A., De Andrade, A., Garcia-Segura, S., Pipi, A., 2019. Electrochemically-driven mineralization of reactive blue 4 cotton dye: on the role of in situ generated oxidants. J. Electroanal. Chem. 840, 415–422.
Oturan, N., Hamza, M., Ammar, S., Abdelhédi, R., Oturan, M., 2011. Oxidation/mineralization of 2-nitrophenol in aqueous medium by electrochemical advanced oxidation processes using pt/carbon-felt and bdd/carbon-felt cells. J. Electroanal. Chem. 661, 66–71.
Ouarda, Y., Bouchard, F., Azaïs, A., Vaudreuil, M.A., Drogui, P., Dayal Tyagi, R., Sauvé, S., Buelna, G., Dubé, R., 2019. Electrochemical treatment of real hospital wastewaters and monitoring of pharmaceutical residues by using surrogate models. Journal of Environmental Chemical Engineering 7.
Palma-Goyes, R., Guzmán-Duque, F., Peñuela, G., González, I., Nava, J., Torres-Palma, R., 2010. Electrochemical degradation of crystal violet with bdd electrodes: effect of electrochemical parameters and identification of organic by-products. Chemosphere 81, 26–32.
Palo, P., Dominguez, J., Gonzalez, T., Sanchez-Martin, J., Cuerda-Correa, E., 2014. Feasibility of electrochemical degradation of pharmaceutical pollutants in different aqueous matrices: optimization through design of experiments. Journal of Environmental Science and Health - Part A Toxic/Hazardous Substances and Environmental Engineering 49, 843–850.
Pang, Y., Abdullah, A., Bhatia, S., 2011. Review on sonochemical methods in the presence of catalysts and chemical additives for treatment of organic pollutants in wastewater. Desalination 277, 1–14.
Panizza, M., Cerisola, G., 2009. Direct and mediated anodic oxidation of organic pollutants. Chem. Rev. 109, 6541–6569.
Panizza, M., Martinez-Huitle, C., 2013. Role of electrode materials for the anodic oxidation of a real landfill leachate - comparison between ti-ru-sn ternary oxide, pbo2 and boron-doped diamond anode. Chemosphere 90, 1455–1460. https://doi.org/10.1016/j.chemosphere.2012.09.006.
Panizza, M., Michaud, P., Cerisola, G., Comninellis, C., 2001a. Anodic oxidation of 2-naphthol at boron-doped diamond electrodes. J. Electroanal. Chem. 507, 206–214.
Panizza, M., Michaud, P., Cerisola, G., Comninellis, C., 2001b. Electrochemical treatment of wastewaters containing organic pollutants on boron-doped diamond electrodes: prediction of specific energy consumption and required electrode area. Electrochem. Commun. 3, 336–339.
Pereira, G., Deroco, P., Silva, T., Ferreira, H., Fatibello-Filho, O., Eguiluz, K., Salazar-Banda, G., 2018. Study of electrooxidation and enhanced voltammetric determination of beta-blocker pindolol using a boron-doped diamond electrode. Diam. Relat. Mater. 82, 109–114.
Punturat, V., Huang, K.L., 2016. Degradation of acesulfame in aqueous solutions by electro-oxidation. Journal of the Taiwan Institute of Chemical Engineers 63, 286–294.
Quesada-Penate, I., Julcour-Lebigue, C., Jauregui-Haza, U.J., Wilhem, A.M., Delmas, H., 2009. Sonolysis of levodopa and paracetamol in aqueous solutions. Ultrason. Sonochem. 16, 610–616.
Raza, N., Raza, W., Gul, H., Kim, K.H., 2021. Zno–znte hierarchical superstructures as solar-light-activated photocatalysts for azo dye removal. Environ. Res. 194 https://doi.org/10.1016/j.envres.2020.110499.
Rodrigo, M., Michaud, P., Duo, I., Panizza, M., Cerisola, G., Comninellis, C., 2001. Oxidation of 4-chlorophenol at boron-doped diamond electrode for wastewater treatment. J. Electrochem. Soc. 148, D60–D64.
Rodrigo, M., Canizares, P., Sanchez-Carretero, A., Saez, C., 2010. Use of conductive-diamond electrochemical oxidation for wastewater treatment. Catal. Today 151, 173–177.
Rovira, J., Domingo, J., 2019. Human health risks due to exposure to inorganic and organic chemicals from textiles: a review. Environ. Res. 168, 62–69. https://doi.org/10.1016/j.envres.2018.09.027.
Sahnoun, S., Boutahala, M., 2018. Adsorption removal of tartrazine by chitosan/polyaniline composite: kinetics and equilibrium studies. Int. J. Biol. Macromol. 114, 1345–1353.
Salazar, C., Contreras, N., Mansilla, H., Yáñez, J., Salazar, R., 2016. Electrochemical degradation of the antihypertensive losartan in aqueous medium by electro-oxidation with boron-doped diamond electrode. J. Hazard Mater. 319, 84–92.
Sathishkumar, P., Mangalaraja, R., Anandan, S., 2016. Review on the recent improvements in sonochemical and combined sonochemical oxidation processes - a powerful tool for destruction of environmental contaminants. Renew. Sustain. Energy Rev. 55, 426–454.
Scialdone, O., Guarisco, C., Galia, A., 2011. Oxidation of organics in water in microfluidic electrochemical reactors: theoretical model and experiments. Electrochim. Acta 58, 463–473.

Sousa, C., Ribeiro, F., Oliveira, T., Salazar-Banda, G., de Lima-Neto, P., Morais, S., Correia, A., 2019. Electroanalysis of pharmaceuticals on boron-doped diamond electrodes: a review. ChemElectroChem 6, 2350–2378.

Srinivasan, S., Sadasivam, S., 2021. Biodegradation of textile azo dyes by textile effluent non-adapted and adapted aeromonas hydrophila. Environ. Res. 194 https://doi.org/10.1016/j.envres.2020.110643.

Tekin, G., Ersöz, G., Atalay, S., 2018. Visible light assisted fenton oxidation of tartrazine using metal doped bismuth oxyhalides as novel photocatalysts. J. Environ. Manag. 228, 441–450.

Thompson, L., Doraiswamy, L., 1999. Sonochemistry: science and engineering. Ind. Eng. Chem. Res. 38, 1215–1249.

Tran, N., Drogui, P., Brar, S., 2015. Sonochemical techniques to degrade pharmaceutical organic pollutants. Environ. Chem. Lett. 13, 251–268.

Urtiaga, A., Perez, G., Ibanez, R., Ortiz, I., 2013. Removal of pharmaceuticals from a wwtp secondary effluent by ultrafiltration/reverse osmosis followed by electrochemical oxidation of the ro concentrate. Desalination 331, 26–34. https://doi.org/10.1016/j.desal.2013.10.010.

Valenzuela, A., Vasquez-Medrano, R., Ibanez, J., Frontana-Uribe, B., Prato-Garcia, D., 2017. Remediation of diquat-contaminated water by electrochemical advanced oxidation processes using boron-doped diamond (bdd) anodes. Water Air Soil Pollut. 228.

Vasconcelos, V., Ponce-de León, C., Rosiwal, S., Lanza, M., 2019. Electrochemical degradation of reactive blue 19 dye by combining boron-doped diamond and reticulated vitreous carbon electrodes. ChemElectroChem 6, 3516–3524.

Vega, L., Soltan, J., Penuela, G., 2019. Sonochemical degradation of triclosan in water in a multifrequency reactor. Environ. Sci. Pollut. Control Ser. 26, 4450–4461.

Vogel, F., Harf, J., Hug, A., Von Rohr, P., 2000. The mean oxidation number of carbon (moc) - a useful concept for describing oxidation processes. Water Res. 34, 2689–2702.

Wachter, N., Aquino, J., Denadai, M., Barreiro, J., Silva, A., Cass, Q., Bocchi, N., Rocha-Filho, R., 2019. Electrochemical degradation of the antibiotic ciprofloxacin in a flow reactor using distinct bdd anodes: reaction kinetics, identification and toxicity of the degradation products. Chemosphere 234, 461–470.

Wang, Y., Zhou, C., Chen, J., Fu, Z., Niu, J., 2019. Bicarbonate enhancing electrochemical degradation of antiviral drug lamivudine in aqueous solution. J. Electroanal. Chem. 848 https://doi.org/10.1016/j.jelechem.2019.113314.

Weng, M., Pei, J., 2016. Electrochemical oxidation of reverse osmosis concentrate using a novel electrode: parameter optimization and kinetics study. Desalination 399, 21–28. https://doi.org/10.1016/j.desal.2016.08.002.

Woisetschlager, D., Humpl, B., Koncar, M., Siebenhofer, M., 2013. Electrochemical oxidation of wastewater - opportunities and drawbacks. Water Sci. Technol. 68, 1173–1179. https://doi.org/10.2166/wst.2013.366.

Zhang, C., Jiang, Y., Li, Y., Hu, Z., Zhou, L., Zhou, M., 2013. Three-dimensional electrochemical process for wastewater treatment: a general review. Chem. Eng. J. 228, 455–467.

Zhao, J., Zhu, C., Lu, J., Hu, C., Peng, S., Chen, T., 2014. Electro-catalytic degradation of bisphenol a with modified co 3o4/b-pbo2/ti electrode. Electrochim. Acta 118, 169–175. https://doi.org/10.1016/j.electacta.2013.12.005.

Zhu, K., Zhu, H., Feng, S., Fu, J., Guo, D., Sun, Q., Huang, L., Hao, X., 2019. Electrochemical Degradation of Chemical Wastewater by Anodic Oxidation Process.

Zollig, H., Remmele, A., Morgenroth, E., Udert, K., 2017. Removal rates and energy demand of the electrochemical oxidation of ammonia and organic substances in real stored urine. Environ. Sci.: Water Research and Technology 3, 480–491. https://doi.org/10.1039/c7ew00014f.